Published in final edited form as:
Anal Chem. 2009 April 15; 81(8): 3001–3007. doi:10.1021/ac802631e.

Determination of ζ-Potential and Tortuosity in Rat Organotypic Hippocampal Cultures from Electroosmotic Velocity Measurements under Feedback Control

Yifat Guy[†], **Robert J. Muha**[†], **Mats Sandberg**[‡], and **Stephen G. Weber**[*,†]
Yifat Guy: yig1@pitt.edu; Robert J. Muha: ; Mats Sandberg: ; Stephen G. Weber:
[†]Department of Chemistry, University of Pittsburgh, Pittsburgh, Pennsylvania 15260
[‡]University of Gothenburg, Gothenburg, Sweden

Abstract

Extracellular translational motion in the brain is generally considered to be governed by diffusion and tortuosity. However, the brain as a whole has a significant ζ-potential, thus translational motion is also governed by electrokinetic effects under a naturally occurring or applied electric field. We have previously measured ζ-potential and tortuosity in intact brain tissue, however the method was tedious. In this work, we use a four-electrode potentiostat to control the potential difference between two microreference electrodes in the tissue, creating a constant electric field. Additionally, some alterations have been made simplify our previous procedure. The method entails simultaneously injecting two 70 kDa dextran conjugated fluorophores into rat organotypic hippocampal cultures and observing their mobility using fluorescence microscopy. We further present two methods of data analysis: regression and two-probe analysis. Statistical comparisons are made between the previous and current methods as well as between the two data analysis methods. In comparison to the previous method, the current, simpler method with data analysis by regression gives statistically indistinguishable mean values of ζ-potential and tortuosity, with a similar variability for ζ-potential, −21.3 ± 2.8 mV, and a larger variability for the tortuosity, 1.98 ± 0.12. On the other hand, we find that the current method combined with the two-probe analysis produces accurate and more precise results, with a ζ-potential of −22.8 ± 0.8 mV and a tortuosity of 2.24 ± 0.10.

Translational motion of molecules in the extracellular space of functioning tissues is typically viewed as being governed by diffusion and tortuosity.[1] Although not as well studied, electroosmotic effects occur in tissues due to natural processes[2] or experimentally applied fields.[3–9] Electroosmotic flow is the bulk fluid flow created by an electric field in a heterogeneous medium with a non-zero ζ-potential. In the brain for example, fixed charges on cell-surface functional groups and constituents of the extracellular matrix create a ζ-potential.[10] The electroosmotic velocity is governed by the magnitude of the ζ-potential.

In order to determine the electroosmotic velocity in brain tissue, it is necessary to know the ζ-potential. Some methods exist for determining the ζ-potentials of particulate objects (e.g., cells) and film-like objects (e.g., skin). ζ-potentials of particulate objects have been determined by electrophoretic techniques.[11–17] Electroosmotic flow in thin samples, such as plant tissue can be determined by flux through the tissue.[18] Electroosmotic flow is described and quantitated as an influential parameter in transdermal iontophoresis[19–25] and transdermal sampling (reverse iontophoresis[24, 26]). Transport through individual skin pores can be observed by

*Corresponding author. Fax: 412-624-1668. E-mail: sweber@pitt.edu.

applying an oscillating electric potential[27] or by scanning electrochemical microscopy.[25] The experimental arrangement for determining the electroosmotic velocity through pores, such as in skin or leaf epidermis, is simplified by the geometry of these biological film-like samples. A potential difference can be generated across the film-like sample. Electrokinetic phenomena then occurs perpendicular to the film-like sample, carrying fluid from one side of the film-like sample to the other.[18] Quantifying ζ-potential and electroosmotic flow in a heterogeneous tissue matrix, on the other hand, is technically challenging.

We have previously published a method of determining ζ-potential and tortuosity in intact organotypic hippocampal slice cultures (OHSCs) using fluorescent probes.[10] The hippocampus is of great interest because it is the center of spatial learning and memory. Conditions such as Alzheimer's disease and ischemia that occur in this region are particularly devastating. The experimental method places an OHSC on the stage of a fluorescence microscope. The velocities of several fluorescent probes in the tissue experiencing an applied electric field are measured. Relating the measured velocities, which are the sums of the electrophoretic and electroosmotic velocities, to the probes' electrophoretic mobilities in free solution leads to a determination of ζ-potential and tortuosity. While successful, the method is not without drawbacks. The focus of this work is to simplify and reduce the effort required to make these measurements while decreasing or at least not increasing the variability in the previous method.

Potential drawbacks in the previous method include: 1) using agarose gel containing a HEPES buffered salt solution (HBSS) as a contact between the electrodes and brain tissue. The contact between the gel and tissue is difficult to reproduce; 2) measuring, not controlling, the electric field. While the field is apparently constant (measured zone velocity independent of time), it would be better to control the field; 3) using eight probes. Using eight probes was helpful to establish experimentally the predicted linearity in a plot of observed vs. electrophoretic mobilities. Now that the linearity is proven, there is no need to repeat the process. Consequently, it may be possible to use fewer fluorescent probes; 4) using probes of various molecular weights. Using probes of similar composition and molecular weight is preferred because tortuosity is dependent on probe composition and molecular weight.[28–30] In this work, the measured ζ-potential and tortuosity are compared to our previous work to assess accuracy and precision. Furthermore, we compare two data analysis approaches to obtain ζ-potential and tortuosity from measurements using only two probes.

THEORY

We have previously published the general theory for determining ζ-potential and tortuosity.[10] The experimental design relies on fluorescent probes with a range of electrophoretic mobilities. In the work presented here, solutions of fluorescent probes are injected simultaneously in pairs into an OHSC on the stage of an inverted microscope. Under the influence of an electric field applied perpendicular to the optical axis, each fluorescent probe will move by electroosmosis, electrophoresis, or both at an observed velocity, v_{obs}, which is the product of the mobility, μ, and the electric field, *E*. The electroosmotic mobility is called μ_{eo}. Equation 1 defines the relationship between μ_{eo} and ζ-potential, ζ.[31, 32]

$$V_{eo} = -\frac{\varepsilon\zeta}{\eta}E = \mu_{eo}E \tag{1}$$

Equation 1 shows that μ_{eo} is a function of ζ, the viscosity of the medium, η, and the permittivity, ε. The same relationship (with a change in sign) exists for electrophoretic velocity, v_{ep}, and

mobility, μ_{ep}. Thus, an observed mobility, μ_{obs}, is defined by equation 2 for an individual molecule, where λ is the tortuosity[10].

$$\mu_{obs}=\frac{V_{obs}}{E}=\left(1/\lambda^2\right)\left(\mu_{ep}+\mu_{eo}\right)=\left(1/\lambda^2\right)\left(\mu_{ep}-\frac{\varepsilon\zeta}{\eta}\right) \quad (2)$$

One method of analysis, implemented in our prior work, uses linear regression to determine the parameters of interest. A linear regression of μ_{obs} on μ_{ep} yields ζ and λ from the intercept and slope using values of ε and η for water. Another method, which we will call the 'two-probe' method, takes advantage of the fact that we use a solution containing two electrophoretically and spectroscopically different fluorescent probes (1 and 2). Each probe moves independently at an observed mobility. The two probes' observed mobilities, measured simultaneously in one experimental run, are used to calculate a single value of ζ and a single value of λ. Values of ζ and λ are determined as shown in equation 3 and equation 4. Here, the numerical subscripts refer to the two probes.

$$\zeta=\mu_{obs1}\frac{\left(\mu_{ep1}-\mu_{ep2}\right)}{\left(\mu_{obs1}-\mu_{obs2}\right)}-\mu_{ep1}\Big/\left(-\varepsilon/\eta\right) \quad (3)$$

$$\lambda_e=\sqrt{\frac{\mu_{ep1}-\mu_{ep2}}{\mu_{obs1}-\mu_{obs2}}} \quad (4)$$

Reported values for ζ and λ are obtained by averaging the results of the individual, two-probe experiments.

EXPERIMENTAL SECTION

Chemicals and solutions

The culture medium was comprised of Basal medium Eagle (50%), Earl's basal salt solution (20%), horse serum (23%), penicillin/streptomycin (25 units/ml), L-glutamine (1 mM), and D-(+)-glucose (7.5 g/L). All components were acquired from Sigma (St. Louis, MO) and used as received. The culture medium was warmed to 37 °C before use, but otherwise was kept in a refrigerator. D-(+)-glucose (27.5 mM) and $MgSO_4$ (2.7 mM) were added to Gey's Balanced Salt solution (GBSS), all also purchased from Sigma, as were the following: HEPES-buffered salt solution (HBSS) containing (mM): 143.4 NaCl, 5 HEPES, 5.4 KCl, 1.2 $MgSO_4$, 1.2 NaH_2PO_4, 2.0 $CaCl_2$, and 10 D-(+)-glucose. HBSS was prepared with 18 MΩ purified water from a Millipore Synthesis A10 system (Millipore, Billerica, MA), filtered and refrigerated at 2.6 °C. It was warmed to 37 °C before use.

Fluorescent probes, Texas Red dextran conjugate 70 kDa (**TR7**) and Fluorescein dextran conjugate 70 kDa (**Fl7**) were purchased from Invitrogen/Molecular Probes (Eugene, OR). **TR7** and **Fl7** were dissolved in HBSS to make 0.34 mM and 0.67 mM solutions, respectively, then filtered with 13 mm, 0.45 μm PTFE Millex filter units or equivalents (Millipore) and frozen until use. The final solution containing both fluorophores had a concentration of 0.19 mM for **TR7** and 0.29 mM for **Fl7**.

Organotypic hippocampal slice cultures

OHSCs were prepared according to the Stoppini culturing technique with small variations.[33] The procedures below were authorized by the University of Pittsburgh IACUC. Seven-day postnatal Sprague-Dawley albino rats were decapitated and the hippocampi dissected bilaterally. The hippocampi were cut perpendicular to the septo-temporal axis using a McIlwain tissue chopper (The Mickle Laboratory Engineering, Surrey, England) into 500 μm thick slices. The OHSCs were placed on Millicell membrane inserts (Millipore CM), pore size 0.4 μm, over culture medium and incubated in 95% air/5% CO_2 at 37 °C. The cultures are roughly ellipsoidal, with the major axis approximately running from the CA3 to the subiculum.

All OHSCs used for the data reported here were cultured for 3 to 10 days, when the tissue thickness is ~150 μm.[33] Prior to an experiment, the culture medium was replaced with 37 °C GBSS and incubated for 30 minutes. This exchange and incubation was repeated two more times, where the final exchange was with 37 °C HBSS. The following manipulations took place at room temperature. The insert membrane was cut using an X-Acto knife to separate the OHSC and the membrane directly beneath it from the insert, as shown in Figure 1. To facilitate handling of the tissue, a millimeter or two of membrane was left extending along the major axis, and the combined membrane/culture was placed in the apparatus with the major axis parallel to the applied field.

Four-electrode potentiostat

We have converted a three-electrode potentiostat (Princeton Applied Research Model 173, Princeton, NJ) to a four electrode potentiostat using a differential amplifier in order to convert the two measured reference electrode potentials into a single difference potential.[34] This potentiostat is capable of applying up to 100 V between the two ‘counter’ electrodes in our apparatus (described below). To accommodate a high common mode voltage, a high voltage operational amplifier, AD445 (shown as U1 and U2 in Supporting Information Figure S-1) from Analogue Devices (Norwood, MA), with a power supply range of +/− 50 volts was used. The amplifier has a typical input bias current of +/− 1.4 pA and a typical input offset current of +/− 0.2 pA. These amplifiers were connected as buffer amplifiers and were the inputs to an AD629 differential amplifier (U3), also from Analog Devices. The amplifier that consists of U1, U2, and U3 allows a common mode range of +/− 42.5 V. Two reference electrodes were connected to the input ends of the amplifier. The reference electrode closest to the cathode was connected to the negative input end of the U3 differential amplifier by way of the buffer amplifier U1 (AD445). Another AD445, U2, was the buffer amplifier connected to the positive input end of U3 and to the other reference electrode. Buffer amplifiers U1 and U2 were connected to a +/− 45 V HP 6205C Dual DC Power (currently Agilent, Santa Clara, CA). A homemade +/− 15 V DC power supply supplied power to U3. Capacitors were used in the power supplies to remove noise, as shown on the bottom of Figure S-1. The output end of U3 was connected to the reference electrode input of the potentiostat. Platinum electrodes in each reservoir of the cell (described below) were the two counter electrodes. They were connected to the auxiliary and working inputs of the potentiostat. This configuration created a feedback loop such that the potential difference between the sensing regions of the two reference electrodes was constant.

Apparatus for tissue experiments

Illustrated schematically in Figure 1, the cell was manufactured locally using Lucite. The cell was comprised of a narrow, 44 mm long, rectangular channel separating two cylindrical reservoirs (19 mm in diameter and 12 mm deep). Each of the reservoirs contained a tubular platinum electrode (1 mm OD, 0.1 mm wall thickness, and ~3.8 cm long) obtained from Goodfellow (Cambridge, England). The OHSC, already removed from the excess insert membrane as described in a previous section, was placed in the middle of the channel. Electrical

contact between the OHSC and the platinum electrodes was made by filter paper, Grade 1 Whatman (Maidstone, England), soaked with HBSS. A piece of filter paper, with one side in the HBSS reservoir, was laid just over one end of the tissue. The same was done with another strip of filter paper from the other reservoir to the other end of the OHSC, as shown schematically in Figure 1. Two 100 μm (ID) fused-silica capillaries, separated by a fixed distance of 2.5 mm, were used as Luggin capillaries. They were each pulled to a tip of ~20 μm (OD) using a P-2000 capillary puller from Sutter (Novato, CA) and inserted into the ends of the OHSC facing each of the platinum electrodes. HBSS filled the Luggin capillaries and their associated vials. The vials each contained a Bioanalytical Systems Ag/AgCl reference electrode (3 M NaCl, West Lafayette, IN). These reference electrodes were connected to the input ends of the differential amplifier as described previously.

Injection capillary

Using the same capillary puller, a 250 μm (ID) fused-silica capillary was pulled to a tip of ~12 μm (OD). The capillary was lowered perpendicularly into the OHSC with a Sutter (Novato, CA) MP-285 micromanipulator. The distal end of the injection capillary connected to a FemtoJet® express from Eppendorf (Hamburg, Germany), which was pressurized by a compressed nitrogen tank from Valley Natural Gas (Wheeling, WV). The FemtoJet® express was set to deliver an injection pressure of 200 to 300 hPa for 0.2 seconds, with a compensation pressure of 40 to 70 hPa.

Imaging

Imaging of the experiment was done with an inverted IX71 fluorescent microscope with a UPlan Apo 4× objective lens, both Olympus products (Melville, NY), and a charge-coupled device camera (ORCA-285 Hamamatsu, Hamamatsu City, Japan). A DA/Fl/TA-3X-A Triple-band “Pinkel” filter set from Semrock (Rochester, NY), with exciter 1 387 nm, exciter 2 494 nm, exciter 3 575 nm, triple-band dichroic mirror: 394–414 nm, 484–504 nm, 566–586 nm, emitter: 457, 530, 628 nm was used according to the fluorescent properties of the probes. SimplePCI 6.0 software from Compix (Cranberry, PA) was used for image acquisition and processing.

ζ-potential determination

Prior to the start of the ζ-potential measurements, an OHSC is injected with each fluorophore solution separately to set each exposure time using the autoexposure command for a two-color image on SimplePCI 6.0. In preparation for each measurement, a fresh OHSC was prepared and placed in the measuring cell on the stage of the microscope. The tip of the injection capillary was loaded with a solution containing both fluorophores at room temperature. It was lowered perpendicularly ~75 μm (approximately midway) into the new OHSC using the micromanipulator. We estimate that the FemtoJet® express delivered about 60 pL of the solution most of the time. Occasionally, mere placement of the capillary in the tissue delivered a larger quantity of the fluorophore solution through capillary effects. Once the injection was complete, the injection capillary was raised from the OHSC and the Luggin capillaries were lowered into the tissue. The time lag from the injection to the application of the electric field is long enough that convective flow from the injection does not interfere with the electroosmotic flow during the measurement.

An electric field between 320 V/m and 2000 V/m was chosen arbitrarily for each run. This range of values was limited on the low end by the need to measure accurately the motion of the fluorescent zones, and on the high end to avoid electroporation.[35] The potentiostat’s applied voltage was determined based on the chosen field and the 2.5 mm reference electrode spacing. Following application of the potential, one image was acquired every one, five, ten, or twenty seconds. The electric field was measured at the two Luggin capillaries by a multimeter to ensure

that the system was controlling the field accurately. The same was done for the two platinum electrodes in the reservoirs.

Figure 2 shows still images taken at two times during an experiment. The Supporting Information includes unenhanced and enhanced movies showing the fluorophore movement. Positive movement of a fluorophore was defined as movement toward the cathode. Using the imaging software, we determined the velocities of the fluorescent zones as follows. The positions of the zones prior to the application of the field (t=0) are defined by the location of the maximum in fluorescence intensity. We then observed the movement of the zones under the influence of the field (using a software-generated video) to determine the point at which a well-defined zone was discernable from the initial zone, as a considerable amount of fluorescence typically remains at or near the position at t=0. The location at a particular time of the intensity maximum of the moving zone defined the zone velocity (N.B. – a multiple-point approach demonstrating constant velocity was used for 203 measurements in the previous publication[10]). The distance that the zones moved in and experiment varied from about 50 to several hundred μm.

RESULTS

We measured fifty pairs of electroosmotic mobilities (one for each fluorescent probe) in OHSCs. One pair's derived values of ζ-potential and tortuosity (based on equation 3 and equation 4) were obviously outliers ($\zeta = -132$ mV and $\lambda = 8.4$). This pair was not included in the following analysis. We will first compare results (previous vs. current) for the directly observed quantity, μ_{obs}. We then compare results (previous vs. current) for the derived parameters, ζ-potential and tortuosity. Finally, we compare the two data treatments, regression vs. two-probe, using the 'current' data.

Table 1a compares the observed mobilities for each fluorescent probe from the previous experimental method to those of the current method using a Student's t-test. The number of runs is n; t is the Student's t value; and p is the probability that the observed difference (t value) is due to chance alone, also known as the p-value. Table 1b shows the analogous variances, s^2, the degrees of freedom, abbreviated as df, as well as the F statistic, Fs, and its p-value, p. It is worth restating that there are several differences between the previous method and the current method. The statistical testing will determine whether the current, much simpler, method gives acceptably equivalent results (t-test) with no poorer precision (F-test) than the previous method. The t-test in Table 1a shows that for both **Fl7** and **TR7** the null hypothesis, that the two mobilities are the same, should be accepted. Additionally, the change in the method modestly improves the precision in both observed mobilities as shown by Table 1b with p-values of 0.07 for both fluorophores. Thus, the observed mobilities are equivalent to, and perhaps more precisely determined, by the simpler current method than the previous method. An increase in precision is helpful because it reduces the number of experiments required to establish a value of the ζ-potential with a given confidence interval.

A linear regression of μ_{obs} vs. μ_{ep} from the current method (n=98) yields a slope of 0.26 ± 0.03 and a y-intercept of $4.3 \pm 0.2 \times 10^{-9}$ m^2/Vs. The stated errors are the SEMs. The slope is equal to the inverse square of the average tortuosity. Therefore, the average tortuosity is 1.98 ± 0.12 (see Table 2a). Inserting the intercept into equation 2 yields an average ζ-potential of -21.3 ± 2.8 mV. Table 2a shows two-tailed t-test comparisons of ζ-potential and tortuosity determined with the current method vs. the values from the previous method.[10] With probabilities of 0.84 for ζ-potential and 0.26 for tortuosity, we infer statistically indistinguishable values. F-test comparisons, as shown in Table 2b (p-values of 0.60 for ζ-potential and 5.2×10^{-5} for tortuosity), show the variability in ζ-potential is indistinguishable from the previous method's. However, this table shows we have increased the variance in the tortuosity determined by the

current method using linear regression for data analysis in comparison to the previous method (which also used linear regression).

We now turn to a comparison of data analysis methods. This comparison is based only on data from the current method. In the regression analysis, all 98 data are used to find ζ-potential and tortuosity. In the two-probe analysis, 49 values of ζ-potential and tortuosity are averaged. Table 3a displays the results of the two analysis methods, namely linear regression and the two-probe method. The two analysis methods yield statistically indistinguishable values for both ζ-potential and tortuosity, as shown by their p-values of 0.60 and 0.24, respectively. However, the F-tests in Table 3b show that the precision greatly improves with the use of the two-probe analysis.

DISCUSSION

Comparison of methods

We made several alterations to the original experimental setup and procedure to simplify and improve the method of determining ζ-potential and tortuosity in intact OHSCs. One such alteration is the use of HBSS in conjunction with filter paper instead of agarose gel slabs. This eliminates the variability in the contact between the tissue and the agarose and eliminates the potential for variability among agarose compositions. Furthermore, the fluid flows more easily within the filter paper than in the agarose gel. This lower resistance to flow minimizes possible pressure differences. Originally, Ag/AgCl electrodes were inserted into the tissue cultures in the experimental region to measure the electric field during the experiment.[10] These electrodes, although small, were invasive and cumbersome. By replacing them with Luggin capillaries, pulled to a tip, the experimental manipulations become easier. The pulled tips of the Luggin capillaries are smaller (~20 μm OD) than the diameters of the Ag/AgCl electrodes (~100 μm each). Also, the capillaries allow the use of larger, more stable, commercially available (BAS) Ag/AgCl electrodes placed in remote vials. By using larger electrodes, amplifiers demanding larger currents are useable, thus simplifying potentiostat design and decreasing drift due to changes in the reference electrode potential occasioned by the operational amplifier current requirement. Most importantly, these electrodes no longer measure the electric field throughout the experiment, but participate in controlling the field between the capillaries with the use of a four-electrode potentiostat. Controlling the field in this manner reduces the variability in the field throughout the experiment. Lastly, the capillaries are now spaced further apart within the tissue culture, so as not to interfere with the fluorophore migration.

The four-electrode potentiostat replaces the use of a voltage supply and reference electrodes for measurement. A three-electrode potentiostat controls the potential between a working electrode and a reference electrode by applying current through an auxiliary electrode. Coupling a differential amplifier to the reference electrode permits the use of two reference electrodes[34] allowing for the control of a potential difference without the requirement that one of the electrode potentials is zero (ground). In this configuration, the potentiostat controls the potential between the two reference electrodes in a feedback loop. Each reference electrode's sensing point is defined by a Luggin capillary. The Luggin tips are small and do not interfere with the experiment. They are inserted along the major axis of the tissue such that the electric field within the tissue is maintained by current between the counter electrodes. The potentiostat maintains the potential difference between the counter electrodes in a range of 14 to 46 V (depending on the tissue and the field that we are trying to achieve). Therefore, the potential at the reference electrodes can be considerably larger than about 15 V vs. ground. This necessitated the use of amplifiers that can manage a high common mode voltage.

The hippocampus is a highly structured region. There are three areas that contain neuronal cell bodies, and thus show up clearly in images of sections of the hippocampal region, namely, the

CA1, CA3, and the dentate gyrus. From the previous work, we know that there are small differences in ζ-potential and tortuosity among these three regions.[10] Of the 98 measurements in the data set for the current experiments, 26 are in the CA1, 36 are in the CA3, and 36 are in the dentate gyrus. A single-factor (regions) analysis of ζ-potential shows a p-value of 0.1 indicating borderline statistically insignificant differences among the regions. In this paper, we have chosen to ignore those (small) differences, thus including observations from the all the regions in a single data set. As Table 1 shows, the current method yields equivalent results for the experimentally observed quantity (in comparison to the previous method) and it is possibly more precise ($p = 0.07$).

Since the linearity of the relationship between μ_{obs} and μ_{ep} is established for OHSCs,[10] it is simpler to use only two probes for the regression analysis rather than eight probes. The potential disadvantage of the two particular probes used here is their relatively similar electrophoretic mobilities. The electrophoretic mobility range in the previous method is almost six times larger than the range in the current method. The range of the experimentally observed mobilities is similarly reduced by about a factor of six. The smaller range in the current method creates a greater sensitivity to additive random errors in the observed mobility than in the previous method. We are thus concerned about suffering an increase in variability of the ζ-potential and tortuosity because of the lower mobility range. Although two-tailed t-tests of both ζ-potential and tortuosity show that the current method (using only two probes) yields statistically indistinguishable results from the previous method (see Table 2a), the F-test in Table 2b test reveals that the alterations increase the variability of tortuosity. The variability in ζ-potential, however, does not increase. The result that there is no observable change in the error of the ζ-potential is favorable, but the increased variance in the tortuosity is disappointing. Fortunately, the two-probe method of analysis leads to improved precision as discussed next.

According to the two-tailed t-tests in Table 3a, the two-probe analysis is a viable analysis method. The significantly better precision of the two-probe analysis method is a result of reduced variability probably due to differences in tissue cultures. The two-probe procedure measures two observed mobilities in the same conditions, since they are injected simultaneously into the same location on the same tissue culture. The hippocampal formation is a highly structured entity in which there are variations in composition (cell bodies vs. projections) over small (~100 μm) distances. While we attempt to inject the probes into the cell-body-containing parts of the tissue, there is certainly a good chance for variability in this aspect of the measurement. Thus, it is not entirely unexpected to find that the variability in the measurement is reduced with the two-probe approach for data analysis.

Accuracy of the method

As Figure 2 and the video clips in the Supporting Information show, the fluorescent probes not only move linearly in the direction of the electric field, but also the initially well-defined zone disperses as it passes through the tissue. It has been shown by computations relating to capillary electrochromatography that in a packed bed, even with a constant ζ-potential, there is a distribution of velocities because of the locally varying electric field.[36] Over the several minute experimental time, the root mean square diffusion distance based on known diffusion coefficients[28, 37] and tortuosity is approximately 40 – 60 μm. As the observed dispersion is greater than this value, it is unlikely that diffusion plays an important role in the observed processes, at least in the two dimensions defined implicitly in Figure 2. On the other hand, we have observed earlier that the fluorescent probes can reside in the insert membrane below the cultured tissue.[10] This population of probe molecules in the membrane moves very slowly in the electric field. Consequently, the injection site is always visible, as is a tail of fluorophore behind the zone moving in the tissue. The tail arises, we think, from probe diffusing out of the membrane into the tissue and vice-versa.

The only extant value of ζ-potential is the value from the previous method. To the degree that the previous method is accurate, the current method is accurate. Tortuosity has been more widely investigated. The two dextran-conjugated fluorophores, **Fl7** and **TR7**, were chosen and paired because they have the same molecular weight, 70 kDa. Previous research has shown correlations between probe molecular weight, or more properly, hydrodynamic radius, and tortuosity.[10, 30, 38, 39] Using probes with the same molecular weight decreases error in tortuosity resulting from variations in probe radii.[28] As far as we are aware, there are no measurements of tortuosity in OHSC other that the value from the previous method. However, there are values for 70 kDa fluorescent dextran in the cortex of rat. The value of the tortuosity in acute rat cortical slices is 2.25[28]. The value in cortex *in vivo* is 2.68[30]. Values of tortuosity for 3 kDa fluorescent dextran in acute hippocampal slices are lower than comparable values in cortex and neocortex.[1] While there are not enough data for a firm conclusion, it appears that measurements of tortuosity by this method are accurate.

Such measurements could be extendable to *in vivo* conditions. However, several challenges arise in an *in vivo* experiment. The most significant is imaging of a fluorophore that is no longer in an optically thin sample. 'Seeing' the region of interest is essential. Consequently, many *in vivo* diffusion measurements are in the easily accessible cortex.[1] Multiphoton experiments,[40] with currently available fluorescent probes, or the use of near IR probes[41] may be helpful. Injections of the fluorophore remain in the tissue following the conclusion of the experiment. Therefore, the fluorophore must be non-toxic to the animal. In addition, electrodes must be placed appropriately for electroosmotic flow to occur. This would be especially challenging for measurements in the interior of the brain. Current neurosurgical methods use transparent conduits,[42] for example, for endoscopic visualization and manipulation with corresponding instruments to access inner brain regions. Similar arrangements can be imagined for an *in vivo* ζ-potential and tortuosity determination. By slightly changing the approach to using contrast agents instead of fluorescent dextran conjugates, magnetic resonance imaging (MRI) and computed tomography (CT) scans can visualize probe movement without a full craniotomy. Electrodes and the injection capillary would still need to be inserted, but this can be minimally invasive.

In conclusion, the new experimental method reduces the variability of the experimentally measured mobilities. Moreover, the two-probe analysis method is accurate and more precise in determining ζ-potential and tortuosity, while also being simpler than the previous method.

Supplementary Material

Refer to Web version on PubMed Central for supplementary material.

REFERENCES

1. Sykova E, Nicholson C. Physiological Reviews 2008;88:1277–1340. [PubMed: 18923183]
2. Savtchenko LP, Kulahin N, Korogod SM, Rusakov DA. Synapse (New York) 2004;51:270–278.
3. Akaneya Y, Jiang B, Tsumoto T. Journal of Neurophysiology 2005;93:594–602. [PubMed: 15604463]
4. Gluckman BJ, Nguyen H, Weinstein SL, Schiff SJ. Journal of Neuroscience 2001;21:590–600. [PubMed: 11160438]
5. LeBeau FEN, Malmierca MS, Rees A. Journal of Neuroscience 2001;21:7303–7312. [PubMed: 11549740]
6. Lerner EN, van Zanten EH, Stewart GR. Journal of Drug Targeting 2004;12:273–280. [PubMed: 15512778]
7. McCaig CD, Sangster L, Stewart R. Developmental Dynamics 2000;217:299–308. [PubMed: 10741424]

8. Miranda PC, Hallett M, Basser Peter J. IEEE transactions on biomedical engineering 2003;50:1074–1085. [PubMed: 12943275]
9. Stone, TW. Microiontophoresis and pressure ejection. Chichester: Wiley; 1985.
10. Guy Y, Sandberg M, Weber SG. Biophysical Journal 2008;94:4561–4569. [PubMed: 18263658]
11. Badr GG, Waldman AA. International Journal of Neuroscience 1973;6:131–139. [PubMed: 4802462]
12. Brewer GJ. J. Theor. Biol 1980;85:75–82. [PubMed: 7464163]
13. Dunlap CA, Biresaw G, Jackson MA. Colloids and Surfaces, B: Biointerfaces 2005;46:261–266.
14. Guzelsu N, Regimbal RL. Journal of biomechanics 1990;23:661–672. [PubMed: 2384482]
15. Miyake M, Kurihara K. Biochim. Biophys. Acta 1983;762:256–264. [PubMed: 6299389]
16. Omasu F, Nakano Y, Ichiki T. Electrophoresis 2005;26:1163–1167. [PubMed: 15704247]
17. Stoilova S, Kancheva M. Stud. Biophys 1986;113:27–30.
18. Polevoi VV, Bilova TE, Shevtsov YI. Biology Bulletin (Moscow, Russian Federation) 2003;30:133–139.
19. Abla N, Naik A, Guy RH, Kalia YN. Journal of Controlled Release 2005;108:319–330. [PubMed: 16169627]
20. Imanidis G, Luetolf P. Journal of Pharmaceutical Sciences 2006;95:1434–1447. [PubMed: 16724334]
21. Nair V, Panchagnula R. Pharmacological Research 2003;48:175–182. [PubMed: 12798670]
22. Nugroho AK, Li GL, Danhof M, Bouwstra JA. Pharmaceutical Research 2004;21:844–850. [PubMed: 15180344]
23. Pikal MJ. Advanced Drug Delivery Reviews 2001;46:281–305. [PubMed: 11259844]
24. Sieg A, Guy RH, Delgado-Charro MB. Biophysical Journal 2004;87:3344–3350. [PubMed: 15339817]
25. Uitto OD, White HS. Pharmaceutical Research 2003;20:646–652. [PubMed: 12739774]
26. Sekkat N, Naik A, Kalia YN, Glikfeld P, Guy RH. Journal of Controlled Release 2002;81:83–89. [PubMed: 11992681]
27. Miyamoto M, Nakahari T, Yoshida H, Imai Y. Journal of Membrane Science 1989;41:377–391.
28. Nicholson C, Tao L. Biophysical Journal 1993;65:2277–2290. [PubMed: 7508761]
29. Prokopova-Kubinova S, Vargova L, Tao L, Ulbrich K, Subr V, Sykova E, Nicholson C. Biophysical Journal 2001;80:542–548. [PubMed: 11159424]
30. Thorne RG, Nicholson C. Proceedings of the National Academy of Sciences of the United States of America 2006;103:5567–5572. [PubMed: 16567637]
31. Probstein, RF. Physicochemical Hydrodynamics, An Introduction: Second Edition. 1994.
32. Rathore AS, Wen E, Horvath C. Analytical Chemistry 1999;71:2633–2641. [PubMed: 10424160]
33. Stoppini L, Buchs PA, Muller D. Journal of neuroscience methods 1991;37:173–182. [PubMed: 1715499]
34. Samec Z, Marecek V, Koryta J, Khalil MW. Journal of Electroanalytical Chemistry and Interfacial Electrochemistry 1977;83:393–397.
35. Olofsson J, Levin M, Stroemberg A, Weber SG, Ryttsen F, Orwar O. Analytical Chemistry (Washington, DC, United States) 2007;79:4410–4418.
36. Nischang I, Tallarek U. Electrophoresis 2007;28:611–626. [PubMed: 17253632]
37. Thorne RG, Hrabetova S, Nicholson C. Journal of Neurophysiology 2004;92:3471–3481. [PubMed: 15269225]
38. Perez-Pinzon MA, Tao L, Nicholson C. Journal of Neurophysiology 1995;74:565–573. [PubMed: 7472364]
39. Sykova E. Neuroscience (Oxford) 2004;129:861–876.
40. Maiti S, Shear JB, Williams RM, Zipfel WR, Webb WW. Science (Washington D. C.) 1997;275:530–532.
41. Pellegatti L, Zhang J, Drahos B, Villette S, Suzenet F, Guillaumet G, Petoud S, Toth E. Chemical Communications (Cambridge, United Kingdom) 2008:6591–6593.
42. Kassam Amin B, Engh Johnathan A, Mintz Arlan H, Prevedello Daniel M. Journal of neurosurgery 2009;110:116–123. [PubMed: 18950265]

ACKNOWLEDGMENT

The authors gratefully acknowledge funding from the National Institutes of Health (R01 GM 44842) and the Swedish Research Council/Medicine.

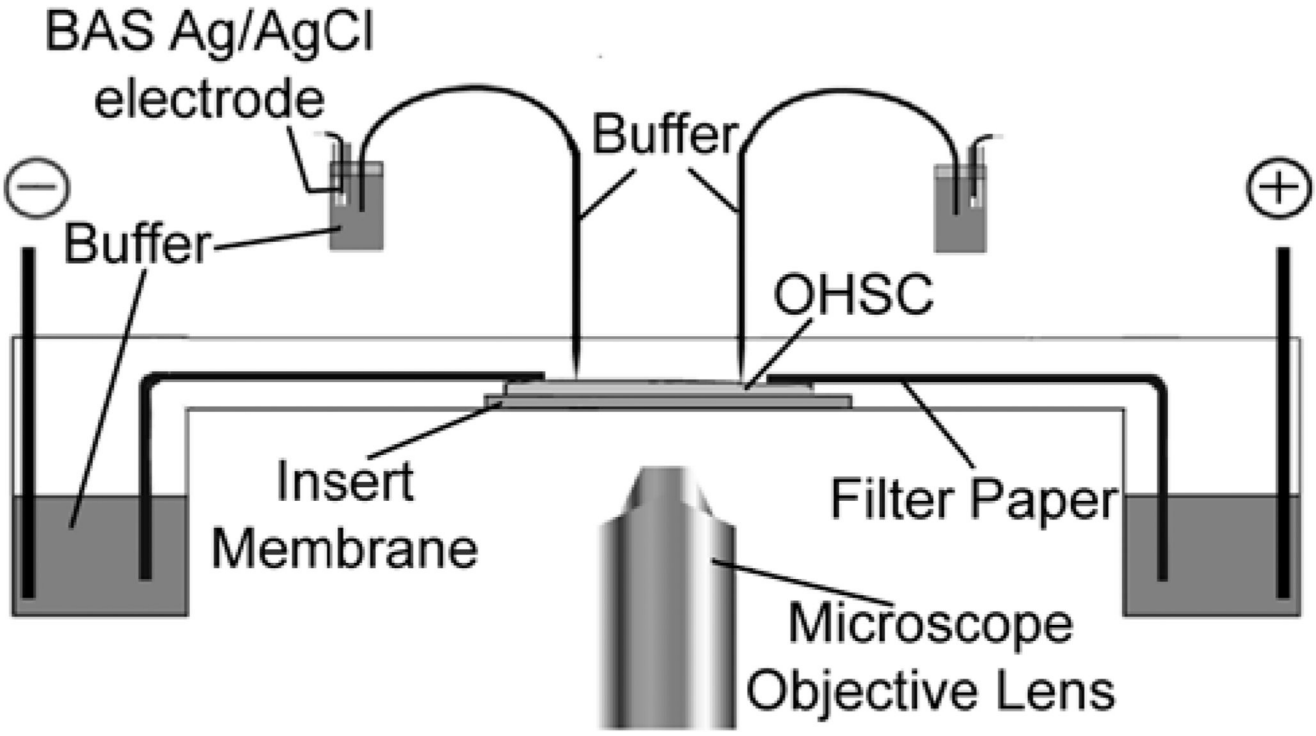

Figure 1.
The apparatus. The apparatus sits on an inverted fluorescence microscope for image analysis. Reservoirs on either side of the apparatus each contain a platinum counter electrode (labeled '−' and '+') and is half filled with HBSS. A HBSS-saturated piece of filter paper spans from inside each reservoir to either end of the OHSC, which sits on a piece of membrane in the center of a channel. Pulled Luggin capillaries are inserted into the OHSC 2.5 mm apart. The distal ends of the capillaries are in vials containing Ag/AgCl electrodes filled with HBSS.

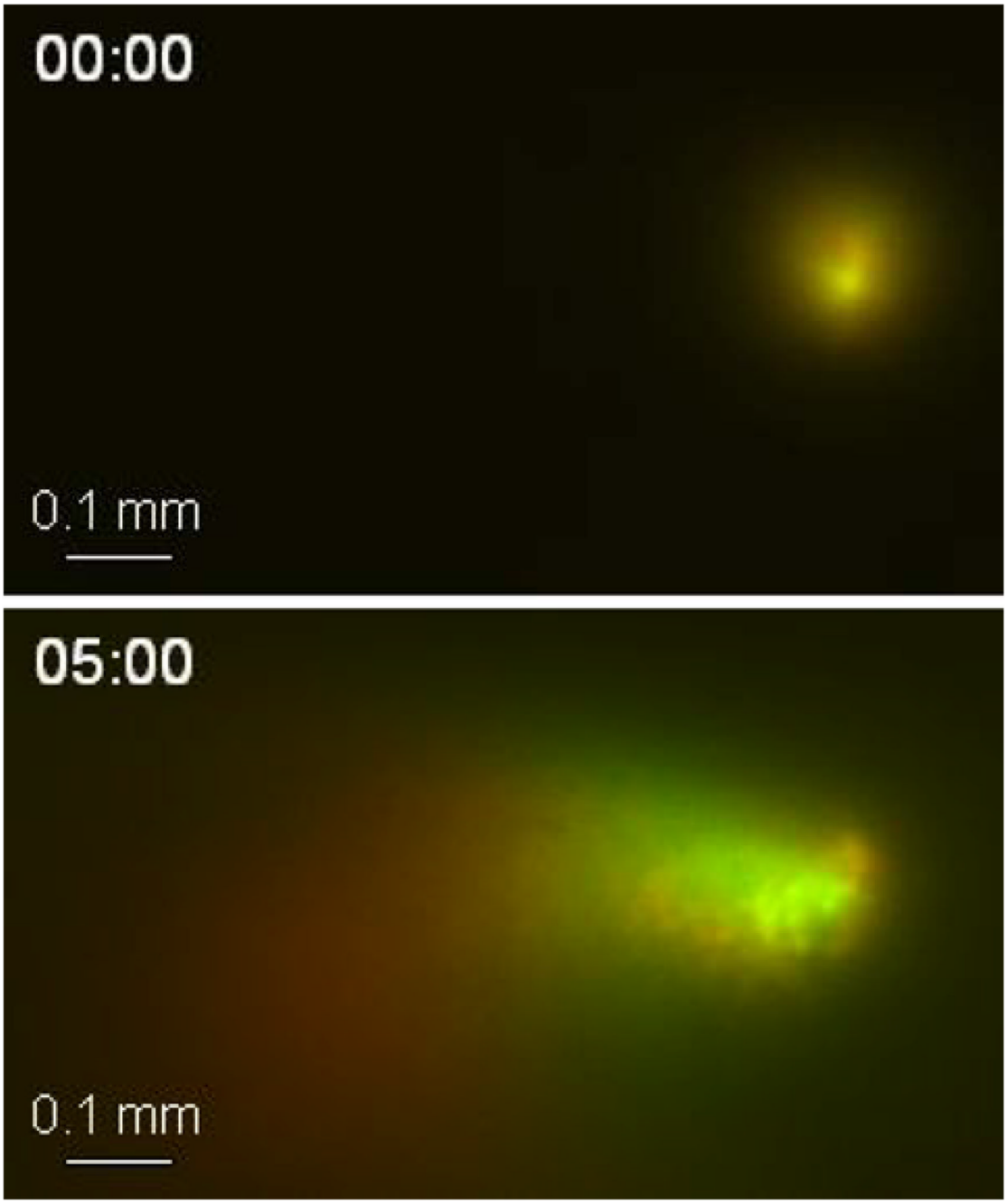

Figure 2.
Sample experimental run. The two images show both fluorophores injected into the CA1 of the OHSC. **TR7** is red, and **Fl7** is green. The top image is taken at time 0. The bottom image shows, at a time of 5 minutes, that the probes have moved towards the cathode. The bottom image's contrast has been increased to increase the visibility of the fluorophores.

Table 1

a. Comparison of observed mobilities

	Previous Method			Current Method				
	μ_{obs} †	SEM†	n	μ_{obs} †	SEM†	n	t	p
Fl7	1.85	0.24	22	1.76	0.13	49	0.40	0.69
TR7	3.66	0.71	12	4.12	0.26	49	0.88	0.38

b. Comparison of variances

	Previous Method		Current Method			
	s^2‡	df	s^2‡	df	F_s	p
Fl7	1.32	21	0.78	48	1.69	0.07
TR7	6.10	11	3.24	48	1.88	0.07

† Units: 10^{-9} m^2/Vs

‡ Units: 10^{-18} m^4/V^2s^2

Table 2

a. Comparison of ζ-potential and tortuosity of the two experimental methods

	Previous Method			Current Method				
	Mean*	SEM*	n	Mean*	SEM*	n	t	p
ζ	−22	2	203	−21.3	2.8	98	0.20	0.84
λ	1.83	0.06	203	1.98	0.12	98	1.1	0.26

b. Comparison of variances

	Previous Method		Current Method			
	$s^{2\S}$	df	$s^{2\S}$	df	F_s	p
ζ	812	201	773.82	96	0.95	0.60
λ	0.73	201	1.42	96	1.93	5.2×10^{-5}

*Units: for ζ, mV; for λ, unitless

§Units: for ζ, mV^2; for λ, unitless

Table 3

a. Comparison of ζ-potential and tortuosity of the two analysis methods

	Regression Analysis			2-Probe Analysis				
	Mean*	SEM*	n	Mean*	SEM*	n	t	p
ζ	−21.3	2.8	98	−22.8	0.8	49	0.52	0.60
λ	1.98	0.12	98	2.24	0.10	49	1.18	0.24

b. Comparison of variances

	Regression Analysis		2-Probe Analysis			
	$s^{2\S}$	df	$s^{2\S}$	df	F_s	p
ζ	773.82	96	29.48	48	26.2	< 0.0001
λ	1.42	96	0.52	48	2.74	0.0001

*Units: for ζ, mV; for λ, unitless

§Units: for ζ, mV^2; for λ, unitless